


REVIEW ARTICLE

A dual-drive four joint time-sharing control walking power-assisted flexible exoskeleton robot system

Jinke Li^{1,2,3,*} , Yong He^{1,2,3}, Jianquan Sun^{1,2}, Pengfei Li^{1,2} and Xinyu Wu^{1,2}

¹Guangdong Provincial Key Lab of Robotics and Intelligent System, Shenzhen Institute of Advanced Technology, Chinese Academy of Sciences, Shenzhen 518055, China, ²Shenzhen Institute of Advanced Technology, Chinese Academy of Sciences, Shenzhen 518055, China, and ³Shenzhen College of Advanced Technology, University of Chinese Academy of Sciences, Shenzhen 518055, China

*Corresponding author. E-mail: jk.li@siat.ac.cn

Received: 30 October 2021; **Revised:** 28 April 2022; **Accepted:** 9 May 2022; **First published online:** 10 June 2022

Keywords: walking analysis, dual-drive four joint, time-sharing control, flexible exoskeleton, metabolic rate

Abstract

Exoskeleton robot can assist people and reduce energy consumption when they walk with heavy weight, so as to protect their health and travel longer distances. This work analyzes the cross gait during walking and designs a dual-drive four joint time-sharing assistance exoskeleton system, which controls the four joints through two motors to realize the assistance to the wearer's movement process. The control curve and adaptive control algorithm are designed to help different people with various walking gaits and speeds, the effectiveness of exoskeleton system is proved by testing metabolism. When the exoskeleton wearer carries 25 kg weight (load equal to 36% of body mass) and travels at the average speed of 5 km/h, the metabolic rate of the exoskeleton wearers decreases by an average of 7.79%, the reduction magnitude is comparable to the effect of taking off 7.33 kg during walking.

1. Introduction

In recent years, lower limb exoskeletons (LLEs) [1, 2, 3] has attracted the attention of many researchers. It plays an important role in rehabilitation [4, 5], power assistance [6, 7] and other fields. Specially, walking assistance is an important research branch of exoskeleton robot, various walking assistance exoskeleton robots [8, 9, 10] have been proposed over the past decades, Which can be mainly divided into two categories: rigid and flexible.

Rigid exoskeleton mainly relies on transferring the weight to the ground to achieve the effect of power assistance, which could load heavy weight. Moreover, due to the structural design, at least one motor need to be used to control one joint. The research group of the university of California Berkeley proposed Berkeley Lower Extremity Exoskeleton [11] and Human Universal Load Carrier [12] in the 2004 and 2007, respectively. These two exoskeleton robots are powered and are driven by the combination of hydraulic and electric, they used four motors to assist ankles and hips. The above exoskeleton robots are powered, there are also some unpowered exoskeleton systems. For example, Collins et al. [?] designed a passive ankle exoskeleton, which is mainly composed of frame, spring and passive clutch. The spring device parallel to the calf gastrocnemius muscle is used to store and release energy when the wearer walks.

However, due to the limitation of mechanical structure, rigid exoskeleton robot will inevitably produce some interference to human action at some time, and the number of active rigid exoskeleton drivers and joints must be the same. Moreover, rigid structures may add large inertia to lower limb of the wearer, which could increase energy consumption during walking [14].

Flexible exoskeleton [15, 16, 17] mostly transfers force through flexible materials such as cables or pneumatic muscles. This kind of exoskeleton usually can not load the weight directly, it depends on

the own bones of wearer to support the weight. In the process of walking, it pulls the joints of lower limbs, so as to achieve the purpose of walking assistance. Italian Institute of Technology [18] designed the exoskeleton based on the pneumatic, which significantly reduces the weight of the system, but it is hard to control accurately. Since 2011, Harvard University has developed SoftExo [19] series flexible exoskeleton robots, which mainly used elastic knitted fabrics as straps and Bowden wires to transfer force. They recognized the motion intention of wearer by Inertial Measurement Unit (IMU) and tension sensor, they pulled wearer's different joints by torque control, including ankle, knee and hip, which could reduce the net metabolic cost by 9.3%. Xosoft proposed by Ortiz et al. [20] realized power assistance through elastic band and clutch, which can provide assistance for the flexion of hip and knee joints. In addition, a new capacitive pressure sensor is used to detect the intention of the wearer and the state of the exoskeleton. Zhang [21] and Ding [22] used two motors to assist hips, they presented the human-in-the-loop control method, this method added human state as feedback to the control algorithm and achieved great success, it can reduce the net metabolic cost by 17.2%. However, it required a respiratory interface computer all the time, which cannot be used in the field for a long time. The above exoskeletons all use a motor to control a joint and do not test the performance under load. Panizzolo [26] presented a multi-joint soft exosuit that can reduce the energy cost by 7.3% with loaded walking.

The aim of this work is to assist more motions and carry load. We analyze the cross swing of legs during walking and design a dual-drive four joint time-sharing control walking assisted flexible exoskeleton robot system, this design adopts two motors to drive four joints. Then, we define a boost curve and trigger based on position control. Besides, we add iterative learning control (ILC) [23] to fit different speeds and gaits.

2. Walking analysis and structure description

2.1. Walking assistance analysis

Human walking is a precise movement process. Walking gait is generally divided into swing phase and support phase, as shown in Fig. 1. For example, when preparing to swing the left leg, the muscle force points of the body are the left calf and the right hip. Therefore, we can choose the heel and hip as the power points of the exoskeleton. Moreover, the most appropriate moment to assist is when the swinging leg begins to swing.

We place four IMUs in the human body to collect the angle information during walking for analysis. Because the two legs are symmetrical, the signs of the values we get are opposite. We define four angles, $Angle_{LA}$ and $Angle_{RA}$ represent the angle of left angle and right angle, respectively. Similarly, $Angle_{LH}$ and $Angle_{RH}$ are the angle of left hip and right hip. The angles of the ankle are based on the transverse plane, and the angles of the hip are based on the coronal plane. These four angles are zero when the wearer is in an upright position. We record these four angles during walking, as shown as Fig. 2. The ranges between the two green lines represent the power range of the right ankle and right hip, and the ranges between the two purple lines represent the power range of the left ankle and left hip. The two legs swing cross in the process of walking, so there is an interval in the time of muscle force. Moreover, the flexible exoskeleton robot has no restriction on the rigid exoskeleton structure, it is feasible to drive the left and right joints with one motor.

2.2. Structure description

In this article, we design a soft exoskeleton robot system as shown in Fig. 3. This system contains six components:

- 1) Actuators, there are two actuators in total, 1) and the motor of each actuator drives two joints through forward rotation and reverse rotation. Conventional permanent magnet motor has large mass, easy saturation of tooth root, serious cogging torque, large positioning torque, large starting

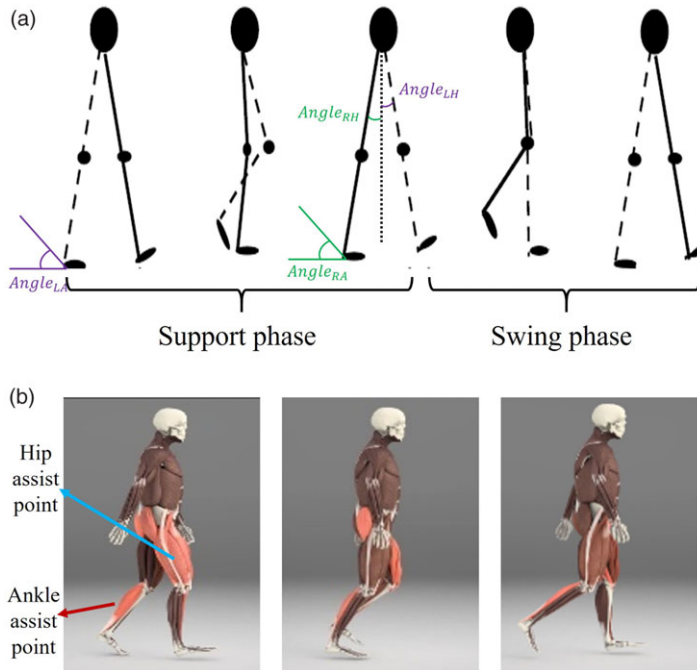


Figure 1. Analysis of walking: (a) Gait cycle and definitions of angles. There are four angles here, which are measured by IMUs and can help us to identify the movement states of the wearer. (b) Analysis of muscle force and selection of assist points during walking, the most appropriate moment to assist is when the swinging leg begins to swing.

current and large rotor inertia, so it is not suitable for frequent start and stop. The rotor of disc motor is a disc structure with permanent magnet. Its unique disc coil structure greatly reduces the volume and weight of the motor. The special inverter device makes it have higher efficiency and greater power than ordinary motors, and can meet higher technical requirements. Therefore, we use two disc motors as the core of the actuators.

The drive system adopts actuator and execution separation structure to transmit power through Bowden cables. The motor pulls the left and right hip joints or ankle joints in forward and reverse directions. The driving unit adopts the structure that the motor drives the winch to wind the steel wire rope and pull the corresponding joint. In order not to interfere with the normal movement of people, the empty stroke of the structural design part is implemented. Under normal circumstances, the steel wire rope is in a relaxed state and the free movement is not affected. If the steel wire rope is fixed to the winch, the steel wire rope will be wound at the outlet due to the reverse rotation of the winch and the relaxation of the steel wire rope, which will affect the release of the steel wire rope. The steel wire fixing block on the winch is designed into a hollow structure, and the steel wire can slide in the hole, which solves the problem of the influence of the rapid movement of the winch on the steel wire.

The winch frame is designed as a groove structure. When relaxed, the steel wire rope will move in series along the axis of the winch. The steel wire rope is easy to get stuck in the gap between the winch and the winch frame, increasing the friction and squeezing the steel wire rope. The groove structure of the disc frame keeps the steel wire rope in the groove all the time, which solves the problem of string movement of the steel wire rope.

- 2) Straps. Straps need to meet three conditions. First, the force points carrying the power, and the relative movement between the force points and the human body shall be avoided as far as possible.

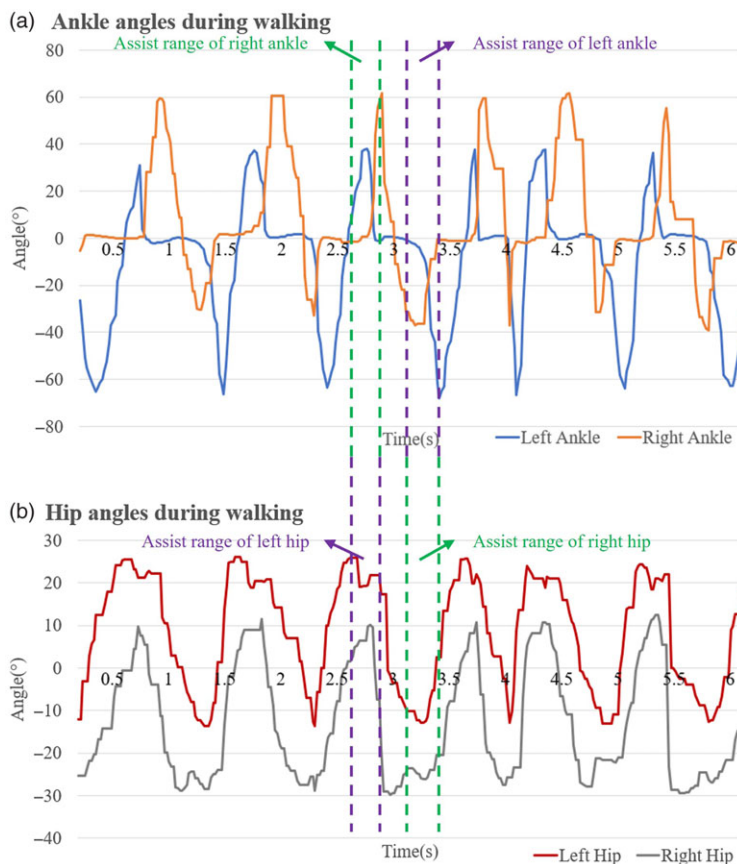


Figure 2. Analysis of gait and assist process. Through these curves, we can find that the assist time at the symmetrical position of both legs is staggered, so we can solve the problem through the forward and reverse rotation of a motor. At the same time, we determine the assist area and assist time point.

Secondly, the system does not interfere with the normal movement of the wearer. Finally, it has high strength, avoids deformation during power assistance and can be used for a long time. There are our parts of straps in total:

- Belt. The belt is the most important support structure in the whole straps structure, which could fix the exoskeleton on the wearer. Moreover, the belt bears the four force loading points of the flexible exoskeleton. The three-dimensional tailoring allows the belt to fit as closely as possible to the wearer's body and to disperse the pressure;
- Hip strap. Hip strap is fixed to the hip. The boost points of the hip are on the hip straps, through which the exoskeleton assists the wearer's hips during walking. Moreover, the IMU is fixed by the hip strap, which could measure the rotation angle of hip.
- Calf strap. Calf strap is fixed to the calf. The main function of the calf strap is to protect the calf, as well as avoiding the lateral movement of the heel assist point.
- Ankle strap. Ankle strap is fixed to the ankle and heel. The ankle strap includes two parts, the upper part is connected with the belt, and the lower part of the ankle strap is connected with the upper part through adjustable nylon buckle, so as to be suitable for wearers of different shapes. It is adjustable, and the main material is nylon. The IMU is fixed in the lower part of the ankle strap, the position of the heel, so that the rotation angle of the ankle can be measured.

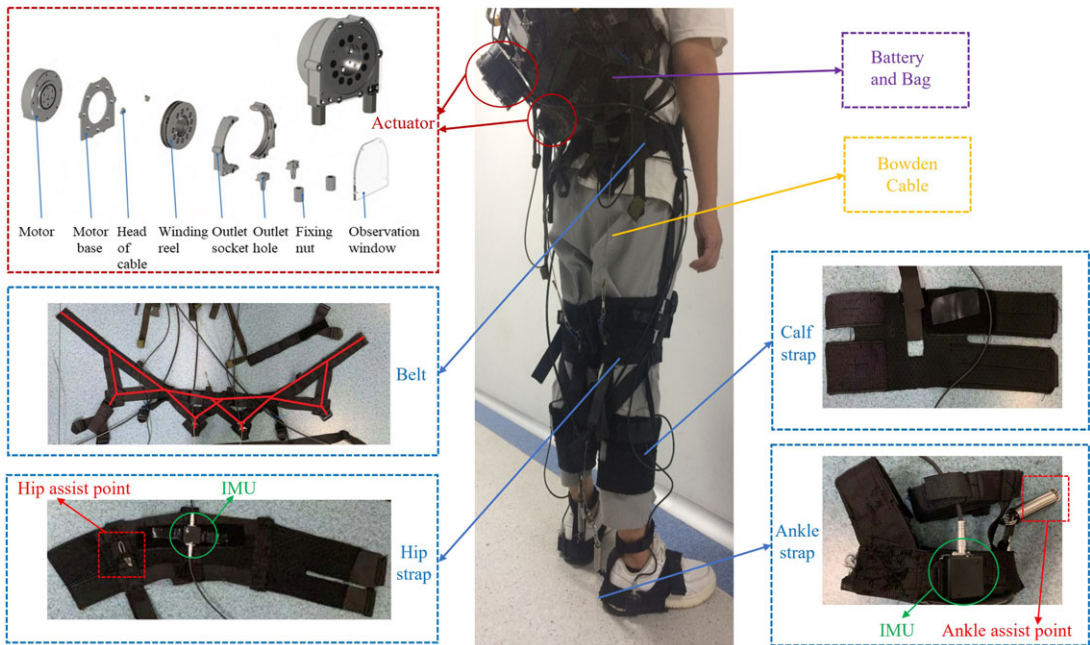


Figure 3. The overview of structural design of the soft exoskeleton robot. It contains six parts, among which straps contain four parts, and their fixed positions and detailed structures are given.

- 3) Bowden cables. Bowden cables are used to transfer force, which connect the actuators to the force points. We wrap a circle of rubber on the Bowden cables to reduce the friction and discomfort of the Bowden cables in direct contact with the human body. The whole exoskeleton system is flexible and cannot be used for kinematic modeling. We directly transmitted the rotation of the motors to the assist points of hip and ankle through Bowden cable. The displacements of the assist points are consistent with the rotation of the motors.
- 4) IMUs. There are four IMUs on the exoskeleton, two per leg, located at the hip and heel, as shown in Fig. 3. The measured values can directly reflect the angles of hip and ankle without conversion. They are used to measure and record the swing angles of the wearer's hips and ankles during walking. Moreover, we used the IMUs to identify the movement states of the wearer. The model of IMU is "HFI-A9", the dynamic accuracy is 0.5° , and the maximum sampling frequency can reach 300 Hz.
- 5) Bag. Bag is used to load heavy objects and fix actuators.
- 6) Battery. The battery provides a power source for the exoskeleton, which can provide 4 h of endurance when traveling at a speed of 5km/ h with a load of 25 kg.

3. Method

3.1. Data preprocessing

Because our exoskeleton system needs to be used independently, we cannot add an additional external motion capture system. Therefore, we use the values of four IMUs as our signal sources to measure the angles of the hip and ankle. The IMUs are fixed on the side of hip and heel, as shown in Fig. 3. The measured values can directly reflect the angles of hip and ankle without conversion.

However, there are always various noises in the sensor signal, so it is necessary for us to filter these data. In order to make the data more smooth and stable, we first add a sliding window filter to the data:

$$Angle_i = \begin{cases} \sum_{n=1}^i Angle_n/i, & 0 < i < 5 \\ \sum_{n=i-4}^i Angle_n/5, & i \geq 5 \end{cases} \tag{1}$$

where $Angle_i$ is the i -th data we get. In this paper, we set the parameter of sliding window filter to 5, which can be adjusted according to different systems and data sampling frequency. Then, we calculate the standard deviation s_i of these data:

$$s_i = \begin{cases} \sqrt{\sum_{n=1}^i (Angle_n - Angle_i)^2/i}, & 0 < i < 5 \\ \sqrt{\sum_{n=i-4}^i (Angle_n - Angle_i)^2/5}, & i \geq 5 \end{cases} \tag{2}$$

On this basis, we add a double mean square deviation filter, which can eliminate some data mutation points:

$$Angle_i = \begin{cases} Angle_{i-1}, & Angle_i < Angle_{i-1} - 2s_{i-1} \text{ or} \\ & Angle_i > Angle_{i-1} + 2s_{i-1} \\ Angle_i, & \text{otherwise} \end{cases} \tag{3}$$

After the above series of data processing, we eliminate the mutation points of the data to ensure the smoothness and stability of the data.

3.2. Assist trigger

In order to calculate the value of A_t , we define the velocity of IMU value as v_{imu} :

$$v_{imu} = \begin{cases} 0, & i = 1 \\ \frac{Angle_i - Angle_{i-1}}{t_{sample}}, & i > 1 \end{cases} \tag{4}$$

Similarly, we define $v_{la}, v_{ra}, v_{lh}, v_{rh}$ as the velocity of the IMU value of left ankle, right ankle, left hip and right hip, respectively. So we can calculate the A_t :

$$A_t = \begin{cases} 1, & Angle_{RA} \cdot Angle_{LH} > 0 \quad \& \quad v_{ra} > 0 \\ -1, & Angle_{LA} \cdot Angle_{RH} > 0 \quad \& \quad v_{la} < 0 \\ 0, & \text{otherwise} \end{cases} \tag{5}$$

where A_t represent the assist state, if $A_t = 1$, the right ankle and left hip begin to assist; if $A_t = -1$, the left ankle and right hip begin to assist; if A_t is 1 or -1 , we set the time point as T_{start} , which means the exoskeleton begins to assist.

3.3. Control curve

The control curves of the four joints are generated in the same way, we take the right leg as an example. According to the different positions of the swinging foot during the movement, we divide the control curve into four parts: $p_{wait}, p_{rise}, p_{stay}$ and p_{back} in this paper. At the same time, we set four time points $T_{wait}, T_{start}, T_{stay}$ and T_{back} to distinguish these parts. As shown in Fig. 4(a):

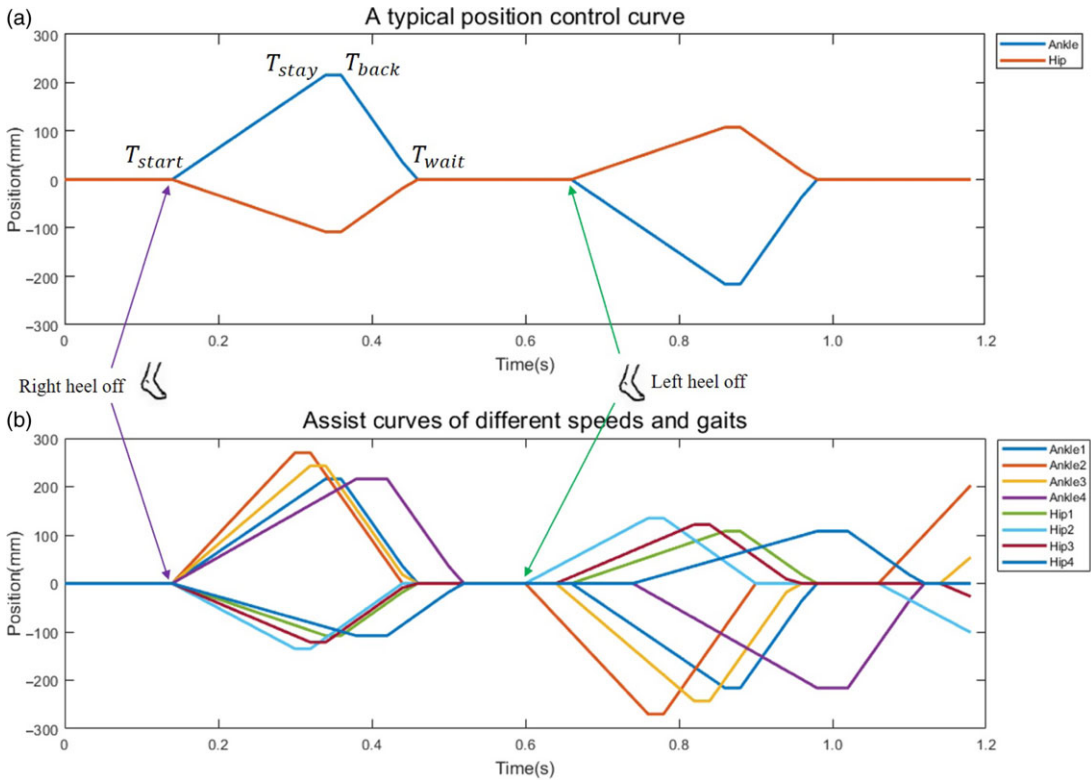


Figure 4. Some possible control curves: (a) A typical position control curve, (b) assist curves of different speeds and gaits. We can completely determine the assist curve according to the calculated T_{start} , T_{stay} and P_{max} .

- 1) $p_{wait}(t)$. From T_{wait} to T_{start} , where T_{start} is the time point that the exoskeleton begins to assist, and T_{wait} is the time point at which the previous control cycle ends. During this time duration, the Bowden cable is loose and the motor remains at zero, so $p_{wait}(t) = 0$;
- 2) $p_{rise}(t)$. From T_{start} to T_{stay} , and:

$$T_{stay} = T_{start} + t_{rise} \tag{6}$$

where t_{rise} is calculated by the previous control cycle. This period of time is the effective assistance period of exoskeleton.

$$p_{rise}(t) = P_{max}/t_{rise}t \tag{7}$$

where P_{max} is the maximum position of motor in this control cycle.

- 3) $p_{stay}(t)$. From T_{stay} to T_{back} , and:

$$T_{back} = T_{stay} + t_{buffer} \tag{8}$$

where t_{buffer} is a defined parameter, it represents the time duration that exoskeleton remains at the maximum position in this control cycle. During this time duration, the Bowden cables are tensioned and the motor remains in the current position, so $p_{stay}(t) = P_{max}$;

- 4) $p_{back}(t)$. From T_{back} to T_{wait} , during this time period, the Bowden cable is loose and the motor goes back to zero point:

$$p_{back}(t) = P_{max} - k_{max}t \tag{9}$$

where k_{max} is the maximum value of motor speed. At this time point, a whole assistance cycle ends.

So the whole position control curve is $p(t)$:

$$p(t) = \begin{cases} 0, & t < T_{start} \\ \frac{P_{max}}{t_{rise}}t, & T_{start} \leq t < T_{stay} \\ P_{max}, & T_{stay} \leq t < T_{back} \\ P_{max} - k_{max}t, & T_{back} \leq t < T_{wait} \end{cases} \tag{10}$$

In this curve, what we need to control are P_{max} and t_{rise} .

We define a parameter c_{system} to reflect the system characteristics of the exoskeleton, which represents the relationship between the motor stretching length $p_{motor}(mm)$ and the joint angle $Angle_{imu}(^\circ)$ measured by IMU. We assume that this is a linear relationship:

$$p_{motor} = c_{system}Angle_{imu} \tag{11}$$

So we can calculate the next $P_{max,m+1}$ by the $m - th$ control cycle:

$$P_{max,m+1} = c_{system}Angle_{max,m} \tag{12}$$

where m represents the $m - th$ control cycle, and $Angle_{max,m}$ is the maximum value of IMU in the $m - th$ control cycle, which can found by peak detection. Besides, we record the time point at which the peak value is reached and set it as $T_{imuMax,m}$, so we can get the next $t_{rise,m+1}$ as

$$t_{rise,m+1} = T_{imuMax,m} - T_{start,m} \tag{13}$$

Because different people have different gaits and walking is a stable and repetitive process, we use iterative learning control (ILC) to calculate P_{max} and t_{rise} :

$$u_m = [P_{max,m} \quad t_{rise,m}]^T \tag{14}$$

$$u_{m+1} = u_m + \beta \cdot e_m \tag{15}$$

where e_m is the error in the $m - th$ control cycle, and \cdot is the iteration parameter, which is a constant in this paper, it determines the convergence rate of the system.

In this section, we describe the control curve of the exoskeleton and use ILC to fit different speeds and gaits, as shown in Fig. 4(b).

4. Experiments

The net metabolic cost is widely used to support its efficiency evaluation in the field of exoskeleton robots. We recruit five volunteers to carry out the metabolism rate experiment. As shown in Fig. 5 we conduct the experiments on an indoor treadmill at a average speed of 5 km/h and a load of 25 kg.

In order to measure metabolism, a gas analyzer (cosmod K5, Rome, Italy) is used to measure the concentration and volume of exhaled lung gas, which is mainly composed of carbon dioxide and oxygen. The metabolic rate can also be calculated with the modified Brockway equation [24]. As the following:

$$\Delta H = c_1V_{O_2} + c_2V_{CO_2} \tag{16}$$

where c_1 is 16.89 kJ/l , c_2 is 4.84 kJ/l , and ΔH is the energy rate (kJ/s). The smaller the ΔH , the smaller the consumption of metabolism.

For each participant, we conduct two groups of experiments to measure the breath gas, with exoskeleton and without exoskeleton. Each group of experiments required the wearer to sit 10 min after loading 25 kg, and then travel on the treadmill at the average speed of 5 km/h for 10 min. Keep the treadmill at 4.5 km/h for 30 s, then switch to 5 km/h for 30 s, then switch to 5.5 km/h for 30 s, and finally switch back to 5 km/h for 30 s, the above is taken as a cycle. The two groups of experiments rested for half an

Table I. Comparison of popular portable LLEs.

Research Group	Assistance Mode	Motor Numbers	Load weight (kg)	Net metabolic cost (%)	Device mass (kg)
Ding et al. [22]	Hips	2	0	17.4	1.37
MacLean et al. [25]	Knee	2	18.1	4.2	8.4
Panizzolo et al. [26]	Hips, Ankles	2	23	7.3	6.6
This work	Hips, Ankles	2	25	7.79	6.2
Panizzolo et al. [27]	Hips	Unpowered	0	3.3	0.65
Collins et al. [10]	Ankles	Unpowered	0	7.2	0.91



Figure 5. Some participants carry K5 on a treadmill with a load of 25 kg and walk at an average speed of 5 km/h.

hour. In order to ensure the accuracy of the data, we take the last 8 min of each 10 min for analysis, as shown in Fig. 6. In the next step of processing, we calculate the average of the flow values (ml/min) of oxygen and carbon dioxide in these 8 min as V_{O_2} and V_{CO_2} , respectively.

Using Eq. (16), the power during resting ($P_{resting}$) and walking ($P_{walking}$) can be calculated, and the net metabolic power (P_{net}) can be obtained from these two values. Then, the net metabolic rate (NMR) can be calculated by net power and body weight (m), as follows:

$$NMR = (P_{walking} - P_{resting})/m \tag{17}$$

Figure 7 shows the experimental results of five testers with a bar graph, in which the blue bar represents $P_{resting}$ and the orange bar represents P_{net} , the figure shows the results with and without exoskeleton, respectively. We can see that the five wearers wearing exoskeleton can reduce metabolism by an average of 7.79%.

The comparison of popular portable LLEs is presented in Table I. When comparing the metabolic cost reduction with previous studies, the mass of the exoskeleton itself and the weight of the load need to be considered. Comparing with unpowered devices [10, 11], our exoskeleton is heavier. However, we can load 25 kg and the net metabolic costs reduction obtained are higher (108% and 236%). These results indicate that the unpowered devices are not suitable for heavy load walking. Comparing with [22],

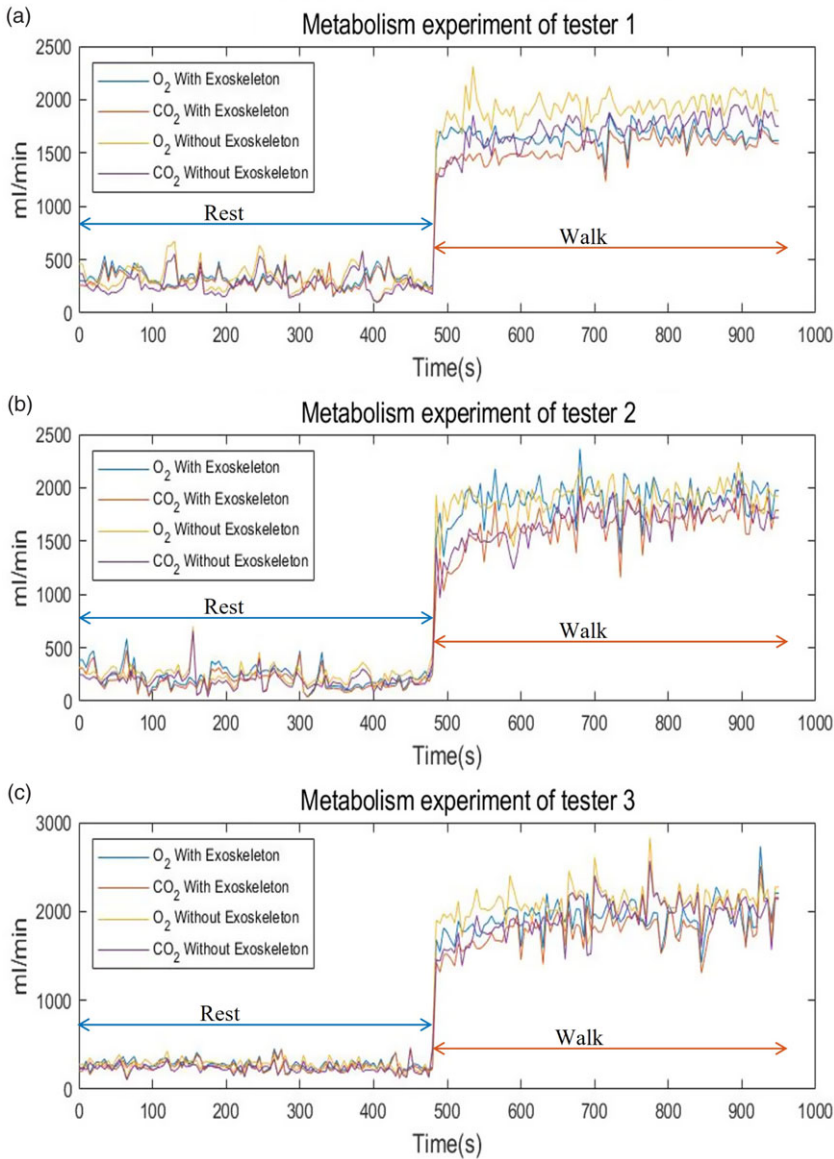


Figure 6. Some of the participants' metabolic results throughout the experiment. The first 8 min are rest, and the next 8 min are walking at an average speed of 5 km/h with a load of 25 kg on the treadmill.

the metabolic cost reduction is lower while the mass is heavier, but it requires a respiratory interface computer all the time, which cannot be used in the field for a long time. Comparing with [26], we all used two motors to drive four joints and loaded about 25 kg, the mass is lighter (94%), while the metabolic cost reduction is higher (107%). Moreover, our exoskeleton could work for 4 h. Therefore, this system is simpler and more efficient.

5. Conclusions and future work

In this work, a soft lower limb exoskeleton (LLE) with active hips assistance and ankles assistance is presented. This design adopts two motors to drive four joints, and the design idea is to assist more motions and carry load. The position control curve based on iterative learning is found suitable to assist

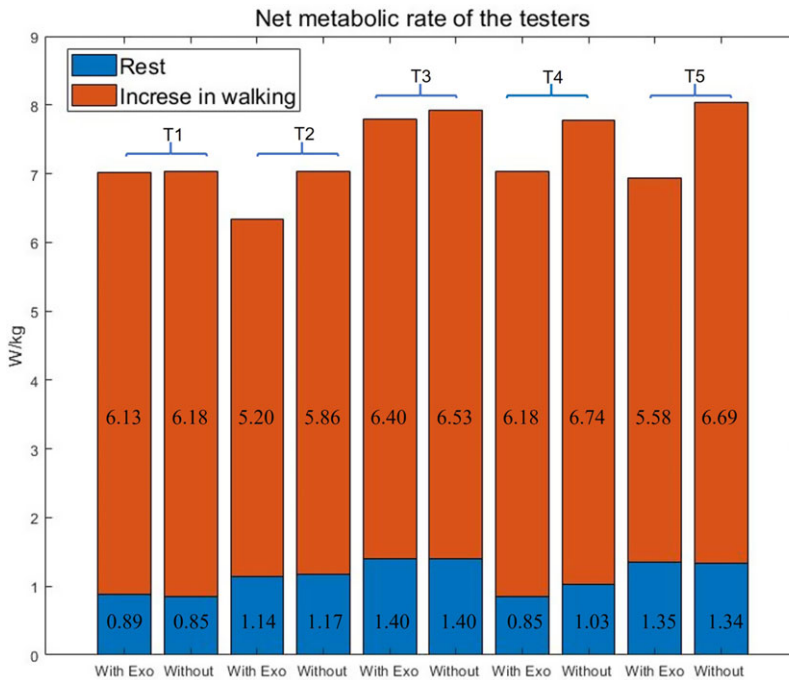


Figure 7. Experimental results of net metabolic rate of the testers. The blue bars are at rest state, and the orange bars are the increased parts when the testers begin to walk at an average speed of 5 km/h with a load of 25 kg on the treadmill. The digits on the column of blue bars mean the net metabolic rate of resting, and the digits on the column of orange bars mean the increased net metabolic rate from rest to walking. T-n represents the results with and without exoskeleton of the n-th tester.

people with different speeds and gaits. The net metabolic costs are reduced when walking at the average speed of 5 km/h with the assistance of the soft LLE.

In future work, the adjustment of control curve will be conducted to improve metabolic reduction. The optimized structure of the exoskeleton will be designed to reduce the weight. The comprehensive evaluation in plateau and different temperature environments will be also conducted.

Authors' contributions. Jinke Li participated in the whole process of this work and wrote the paper. Yong He designed the structure. Jianquan Sun, Pengfei Li and Xinyu Wu processed the exoskeleton system and organized the participants to carry out the experiments.

Financial support. This work was partially supported by the National Natural Science Foundation of China under Grant No. 6212530, in part by the National Natural Science Foundation of China under Grant No.U2013209, and in part by the National Natural Science Foundation of China under Grant No.U1913211.

Conflicts of interest. The authors declare no conflicts of interests.

Ethical considerations. All the subjects signed an informed consent prior to their participation in the experiments. This study was approved by the Medical Ethics Committee of Shenzhen Institute of Advanced Technology (SIAT-IRB-200715-H0512, valid time from 2020.01 to 2022.12).

References

- [1] H. Herr, "Exoskeletons and orthoses: Classification, design challenges and future directions," *J. Neuroeng. Rehabil.* **6**(1), 21 (Jun 18, 2009).
- [2] L. N. Awad, J. Bae, K. O'Donnell, S. M. M. De Rossi, K. Hendron, L. H. Sloop, P. Kudzia, S. Allen, K. G. Holt, T. D. Ellis, C. J. Walsh, "A soft robotic exosuit improves walking in patients after stroke," *Sci. Transl. Med.* **9**(400), (Jul 26, 2017).

- [3] Q. C. Wu, X. S. Wang, B. Chen and H. T. Wu, "Development of a minimal-intervention-based admittance control strategy for upper extremity rehabilitation exoskeleton," *IEEE Trans. Syst. Man Cybern. Syst* **48**(6), 1005–1016 (Jun, 2018).
- [4] A. Esquenazi, M. Talaty, A. Packel and M. Saulino, "The ReWalk powered exoskeleton to restore ambulatory function to individuals with thoracic-level motor-complete spinal cord injury," *Am. J. Phys. Med. Rehabil.* **91**(11), 911–921 (Nov, 2012).
- [5] X. Y. Wu, Y. Ma, X. Yong, C. Wang, Y. He and N. Li, "Locomotion mode identification and gait phase estimation for exoskeletons during continuous multilocomotion tasks," *IEEE Trans. Cognit. Dev. Syst.* **13**(1), 45–56 (Mar, 2021).
- [6] T. Kagawa, H. Ishikawa, T. Kato, C. Sung and Y. Uno, "Optimization-based motion planning in joint space for walking assistance with wearable robot," *IEEE Trans. Robot.* **31**(2), 415–424 (Apr 2015).
- [7] A. T. Asbeck, K. Schmidt, I. Galiana, D. Wagner and C. J. Walsh, "Multi-joint Soft Exosuit for Gait Assistance," **In:** 2015 IEEE International Conference on Robotics and Automation (ICRA) (2015) pp. 6197–6204.
- [8] Di Natali C., Poliero T., Sposito M., Graf E., Bauer C., Pauli C., Bottenberg E., De Eyto A., O'Sullivan L., Hidalgo Aés F., Scherly D., Stadler K. S., Caldwell D. G., Ortiz J. A., "Design and evaluation of a soft assistive lower limb exoskeleton," *Robotica* **37**(12), 2014–2034 (2019).
- [9] L. Rose, M. C. Bazzocchi and G. Nejat, "A model-free deep reinforcement learning approach for control of exoskeleton gait patterns," *Robotica* **9**, 1–26 (2021).
- [10] CaoW., ChenC., WangD., WuX., ChenL., XuT. and LiuJ., "A lower limb exoskeleton with rigid and soft structure for loaded walking assistance," *IEEE Robot. Autom. Lett.* **7**(1), 454–461 (2021).
- [11] A. Zoss, H. Kazerooni and A. Chu, "Hybrid Control of the Berkeley Lower Extremity Exoskeleton (BLEEX)," **In:** 2006 IEEE/Rsj International Conference on Intelligent Robots and Systems (2006).
- [12] K. A. Strausser and H. Kazerooni, "The Development and Testing of a Human Machine Interface for a Mobile Medical Exoskeleton," **In:** 2011 IEEE/Rsj International Conference on Intelligent Robots and Systems (2011).
- [13] S. H. Collins, M. B. Wiggin and G. S. Sawicki, "Reducing the energy cost of human walking using an unpowered exoskeleton," *Nature* **522**(7555), 212–215 (Jun 11, 2015).
- [14] R. C. Browning, J. R. Modica, R. Kram and A. Goswami, "The effects of adding mass to the legs on the energetics and biomechanics of walking," *Med. Sci. Sports Exerc.* **39**(3), 515–525 (Mar, 2007).
- [15] W. Cao, C. Chen, H. Hu, K. Fang and X. Wu, "Effect of hip assistance modes on metabolic cost of walking with a soft exoskeleton," *IEEE Trans. Automat. Sci. Eng. Manuf. Technol.* **18**(2), 426–436 (2020).
- [16] B. Liu, Y. Liu, Z. Zhou and L. Xie, "Control of flexible knee joint exoskeleton robot based on dynamic model," *Robotica* **7**, 1–17 (2022).
- [17] X. Wu, W. Cao, H. Yu, Z. Zhang, Y. Leng and M. Zhang, "Generating electricity during locomotion modes dominated by negative work via a knee energy-harvesting exoskeleton," *IEEE/ASME Trans. Mechatron.*, 1–11 (2022).
- [18] D. G. Caldwell, N. G. Tsagararakis, S. Kousidou, N. Costa and I. Sarakoglou, "'Soft' exoskeletons for upper and lower body rehabilitation – Design, control and testing," *Int. J. Hum. Robot.* **4**(3), 549–573 (Sep, 2007).
- [19] J. Kim, G. Lee, R. Heimgartner, D. A. Revi, N. Karavas, D. Nathanson, I. Galiana, A. Eckert-Erdheim, P. Murphy, D. Perry, N. Menard, D. K. Choe, P. Malcolm, C. J. Walsh, "Reducing the metabolic rate of walking and running with a versatile, portable exosuit," *Science* **365**(6454), 668–672 (Aug 16, 2019).
- [20] J. Ortiz, C. D. Natali and D. G. Caldwell, "XoSoft – Iterative Design of a Modular Soft Lower Limb Exoskeleton," **In:** *Proceedings of the 4th International Symposium on Wearable Robotics, WeRob2018*, Pisa, Italy (October 16–20, 2018).
- [21] J. Zhang, P. Fiers, K. A. Witte, R. W. Jackson, K. L. Poggensee, C. G. Atkeson and S. H. Collins, "Human-in-the-loop optimization of exoskeleton assistance during walking," *Science* **356**(6344), 1280–1284 (Jun 23, 2017).
- [22] Y. Ding, M. Kim, S. Kuindersma and C. J. Walsh, "Human-in-the-loop optimization of hip assistance with a soft exosuit during walking," *Sci. Robot.* **3**(15, Feb 28), 498 (2018).
- [23] D. A. Bristow, M. Tharayil and A. G. Alleyne, "A survey of iterative learning control," *IEEE Control Syst.* **26**(3), 96–114 (2006).
- [24] J. M. Brockway, "Derivation of formulas used to calculate energy-expenditure in man," *Hum. Nutr. Clin. Nutr.* **41c**(6), 463–471 (Nov, 1987).
- [25] M. K. MacLean and D. P. Ferris, "Energetics of walking with a robotic knee exoskeleton," *J. Appl. Biomech.* **35**(5), 320–326 (Oct 1 2019).
- [26] F. A. Panizzolo, I. Galiana, A. T. Asbeck, C. Sivi, K. Schmidt, K. G. Holt and C. J. Walsh, "A biologically-inspired multi-joint soft exosuit that can reduce the energy cost of loaded walking," *J. Neuroeng. Rehabil.* **13**(1), 1–14 (2016).
- [27] F. A. Panizzolo, C. Bolgiani, L. Di Liddo, E. Annese and G. J. J. Marcolin, "Reducing the energy cost of walking in older adults using a passive hip flexion device," *J. Neuroeng. Rehabil.* **16**(1), 1–9 (2019).